

## Observations of Homogeneous Phase Separation in Liquid $^3\text{He}$ - $^4\text{He}$ Mixtures

J. K. Hoffer, L. J. Campbell, and R. J. Bartlett

*Los Alamos Scientific Laboratory, Los Alamos, New Mexico 87545*

(Received 25 February 1980)

This Letter describes the physical behavior of superfluid dispersions created by pressure quenching  $^3\text{He}$ - $^4\text{He}$  mixtures into the miscibility gap. The two types of dispersions, namely, superfluid droplets within a normal-fluid continuous phase and the inverse, evolve differently. Under certain conditions near the tricritical point, light scattering during the early stages of separation displays a halo at a time-dependent wave vector  $k_m \propto t^{-\varphi}$ , where  $\varphi$  shows a crossover from slow ( $\varphi \approx \frac{1}{3}$ ) to fast ( $\varphi = 1$ ) growth within 0.1 s.

PACS numbers: 67.60.-g, 64.70.Ja, 82.70.Kj

The miscibility gap that exists below the tricritical point in liquid  $^3\text{He}$ - $^4\text{He}$  mixtures permits the study of binary phase decomposition and the ensuing dispersions<sup>1</sup> in a system having an additional order parameter in one of the components. This order parameter significantly complicates even a linear description of the separation,<sup>2</sup> and so it is interesting to compare the experimental decomposition with that of normal liquids.<sup>3-6</sup> Moreover, the phase separation curves of  $^3\text{He}$ - $^4\text{He}$  mixtures are highly unsymmetric at the critical point so that critical decompositions lead to coexisting phase proportions of 17-83, rather than 50-50 as in normal liquids. Such decompositions and dispersions are described here for the first time.

The cell was formed by milling a hole 1.59 by 3.81 cm into a 1.59-cm-thick block of copper, and then attaching quartz windows over indium gaskets. This was placed in a  $^3\text{He}$  cryostat having conventional glass Dewars. The mixtures could be pressurized by a vane pump or by a cryogenic intensifier in parallel with the cell. Once pressurized, a mixture could be depressurized by opening a valve leading to a storage tank. The capillary lines to the sample cell were sized large to permit rapid decompression. If limited only by sonic velocities in the 0.2-mm-i.d. connecting capillary, decompression rates could be as high as  $10^2$  atm/s, equivalent to temperature quenching rates approaching 4 K/s.

Wong and Knobler showed that rapid decompression is an effective way to quench isobutyric acid and water mixtures either into<sup>4</sup> or near<sup>7</sup> the miscibility gap. The same can be done in  $^3\text{He}$ - $^4\text{He}$  mixtures, as seen from the phase diagram in Fig. 1.<sup>8</sup> Decompressing equilibrium mixtures at  $P = 5$  atm (open circles) to saturated vapor pressure (SVP) creates momentary nonequilibrium states which evolve toward points on the SVP curves (solid circles). If the initial state consists

of coexisting phases (lower open circles), then each of these will independently decompose, after which gravity will separate the two resulting dispersions into two bulk liquid volumes. The relative fractions of liquid in the  $^3\text{He}$ -rich and  $^4\text{He}$ -rich phases of each dispersion is given by the lever rule applied to the  $^3\text{He}$  concentration of the initial state (open circles). By choosing the total  $^3\text{He}$  concentration to be near the critical concentration it is possible to reach all points (as initial states for quenching) on an isobaric coexistence curve by merely changing the temperature.

We performed quenches from pressures of 6.7 atm or less, at several temperatures from 0.55

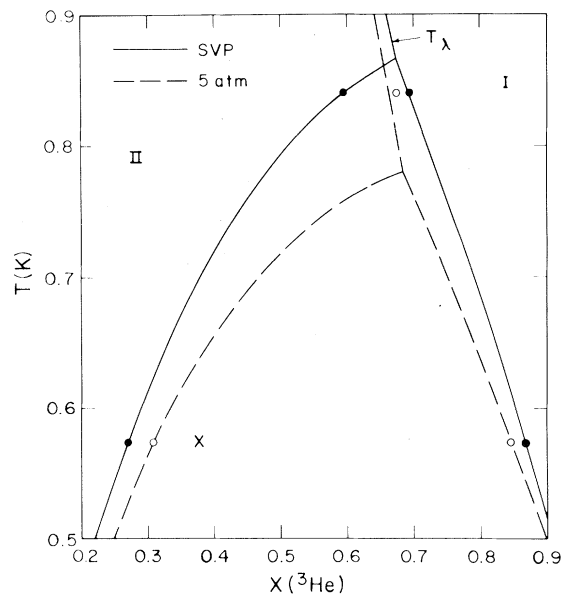


FIG. 1. Miscibility gap between normal (I) and superfluid (II) mixtures of  $^3\text{He}$  and  $^4\text{He}$ . The coexistence curves for 5 atm are approximate. Open dots represent initial states which decompose, upon decompression, into states shown by the solid dots at approximately the same temperature.

K to  $T_t = 0.867$  K, and at total  $^3\text{He}$  molar concentrations  $x$  of 0.25, 0.375, 0.675, and 0.84. Several of these quenches were recorded on film at 50 frames per second. A specific example is the initially phase-separated mixture at  $T = 0.574$  K,  $P = 5$  atm, and  $x = 0.375$ , indicated by the  $\times$  and lower circles in Fig. 1. Upon quenching (to a pressure slightly above SVP) the (upper) normal fluid phase acquires, after a delay of 1 to 2 s, a fine mist of  $^4\text{He}$ -rich droplets, which undergo no appreciable growth as they fall at a uniform speed until they are absorbed at the interface with the superfluid phase. The normal phase clears noticeably from the top downward as the mist settles through it. By contrast, the superfluid phase after decompression immediately becomes cloudy with  $^3\text{He}$ -rich droplets, which grow rapidly. Here the gravitational separation is marked by very turbulent, chaotic motion of the rising droplets. Both normal and superfluid dispersions clear after 3 to 4 s.<sup>9</sup> The droplet velocities were  $4.6 \pm 0.3$  mm/s in the normal dispersion and, initially,  $9.4 \pm 0.3$  mm/s in the superfluid dispersion.

The size of the droplets can be estimated from the equation for the terminal velocity of a spherical drop of viscosity  $\eta'$  moving under gravity in a fluid of viscosity  $\eta$ .<sup>10</sup> Using Kierstead's data<sup>11</sup> for the liquid densities and that of Lai and Kitchens<sup>12</sup> for  $\rho\eta$ , we infer diameters of  $17 \pm 2$   $\mu\text{m}$  for  $^4\text{He}$ -rich droplets in the normal dispersion and  $21 \pm 2$   $\mu\text{m}$  for the  $^3\text{He}$ -rich droplets in the initial superfluid dispersion.

The above description applies to quenches of either homogeneous or phase-separated initial states in other regions of the miscibility gap, except possibly near the tricritical point ( $0.84$  K  $< T \leq T_t$ ) where the vanishing difference between the indices of refraction made visual observations and photographic recording more difficult, even though the time scale increased.

We pass now to light-scattering measurements made during the early stage of phase separation. Huang, Goldberg, and Bjerkaas<sup>3</sup> used a pencil beam of laser light in the first study of binary separation in liquids (methanol and cyclohexane) and observed a halo of increased intensity in the far-field scattering pattern. This halo intensified, contracted, and disappeared over a period of several minutes. We also observe such phenomena, with the notable difference being the collapse of the halo in less than 0.5 s. Figure 2 shows three scattering patterns from a He-Ne laser ( $\lambda = 6328$  Å) during a quench of a homogeneous mixture with  $x = 0.675$ ,  $T = 0.840$  K, and initial

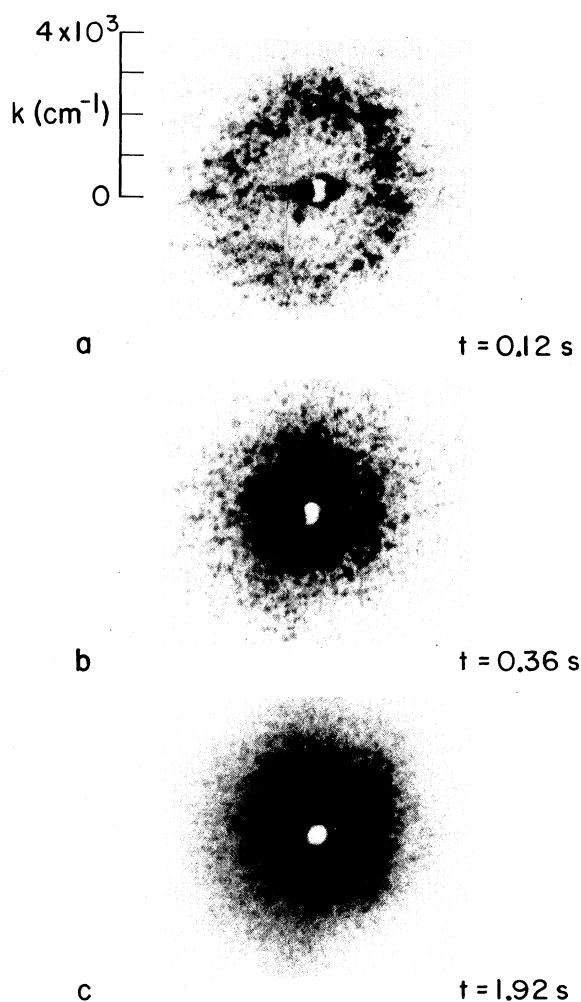


FIG. 2. Far-field scattering of laser beam at three times after decompression from a state represented by the upper open dot in Fig. 1. The center spot is a hole in the screen to pass the undeflected beam.

pressure of 3.7 atm (upper, open circle in Fig. 1). The halo, Fig. 2(a), collapses in 0.3 s to a disk, Fig. 2(b), having a ragged boundary of speckles which fluctuate faster than 0.02 s, the time between movie frames. After about 1.4 s the boundary of the disk becomes diffuse, Fig. 2(c), as a result of multiple scattering from the emerging mist of dispersed phase mentioned above. The appearance and evolution of the halo occurs before noticeable clouding of the sample. Perhaps for this reason, no halos were seen upon quenching superfluid mixtures, for which there is no discernible delay in the appearance of a thick mist. Similar to the findings of Goldberg *et al.*,<sup>5</sup> the undeflected intensity of the beam, as moni-

tored with a photodiode, sharply decreased for about 0.3 s after the quench and then increased slowly, with large fluctuations, to its prequench value.

The wave vector  $k_m$  for maximum scattering intensity decreases with time, as shown in Fig. 3, where the vertical bars denote the approximate width of the halo as it appears on film. The slope of the points at short times is sensitive to our assumption that the quench occurred 0.02 s (one frame) before the first detectable halo. If the quench were actually somewhat earlier it would steepen the slope of the early-time points but would not appreciably affect the slope of the later points, which is essentially unity. Slopes of  $-\frac{1}{3}$  and  $-1$  are indicated as guides. This behavior of  $k_m$  is surprisingly similar to that recently reported by Chou and Goldberg<sup>6</sup> for both isobutyric acid-water and 2,6-lutidine-water. When scaled with the composition diffusivity  $D$  and concentration correlation length  $\xi$ , their data for  $k_m(t)$  for various quenches become closely clustered [Eqs. (4) and (5) and Figs. 4 and 5 of Ref. 6]. Assuming our data should lie in the same cluster implies a ratio of effective diffusion constant to correlation length squared of  $D/\xi^2 \approx 10^3 \text{ s}^{-1}$  for the quench in Fig. 3. This comes from matching the times at the crossover to  $k_m \propto t^{-1}$  behavior. By similarly matching the wave vectors  $k_m$  at crossover we obtain  $\xi \approx 9 \times 10^{-5} \text{ cm}$ . Because the majority phase in this quench was normal, the above  $D$  and  $\xi$  are presumably related more closely to values  $D_+$  and  $\xi_+$  of the normal fluid than to  $D_-$  and  $\xi_-$  of the superfluid. Indeed,  $D_-/\xi_-^2 \approx 10^7 \text{ s}^{-1}$  at  $T = 0.840 \text{ K}$ ,

according to the data of Leiderer and co-workers.<sup>13</sup> (This is consistent with the much faster decomposition seen for superfluid dispersions.) No independent measurements of  $D_+$  and  $\xi_+$  have been reported.

While our results are consistent with  $k_m \propto t^{-1/3}$  at early times, as predicted by several theories,<sup>14</sup> they are not confirming because of the uncertainty in the time of quench. However, the region for  $k_m \propto t^{-1}$  is much more convincing and agrees with arguments of Siggia<sup>15</sup> which depend on widespread connectivity in the minority phase. Although such connectivity is expected in critical quenches resulting in 50-50 phase separation,<sup>6</sup> it is far less obvious in our case where the final separation was closer to 20-80. This suggests there may be another mechanism for the  $t^{-1}$  behavior of  $k_m$ . No other data have been reported for such disparate proportions of the phases.

No halos were observed below 0.75 K, possibly because the only states accessible were metastable rather than unstable (even though separation occurred quickly). This is in rough agreement with the position of the  $C_1$  spinodal line estimated by Hohenberg and Nelson.<sup>2</sup>

We enjoyed helpful conversations with W. I. Goldberg, C. M. Knobler, and P. C. Hohenberg. We wish to thank J. R. Miller for technical advice and Y. Disatnik and R. M. Ziff for earlier contributions.<sup>16</sup> This work was supported by the National Aeronautics and Space Administration working group for Physics and Chemistry in Space (PACE) and the U. S. Department of Energy.

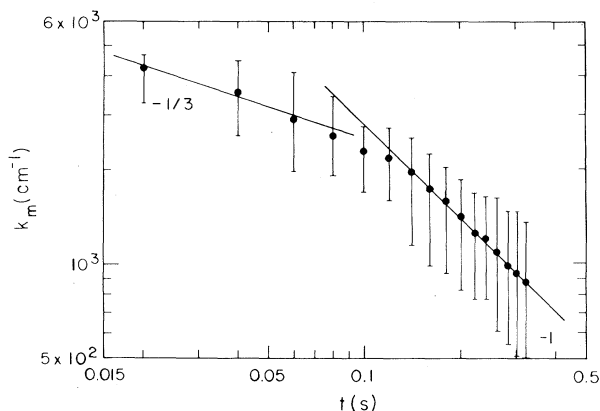


FIG. 3. Wave vector of halo maximum for same quench as shown in Fig. 2. Slopes of  $-\frac{1}{3}$  and  $-1$  are shown for comparison. The vertical lines represent the approximate limits of the halo as recorded on film.

<sup>1</sup>We call a phase-separating system a *dispersion* once the relative volumes of the constituent phases are no longer changing.

<sup>2</sup>P. C. Hohenberg and D. R. Nelson, Phys. Rev. B **20**, 2665 (1979).

<sup>3</sup>J. S. Hunag, W. I. Goldberg, and A. W. Bjerkaas, Phys. Rev. Lett. **32**, 921 (1974).

<sup>4</sup>N. C. Wong and C. M. Knobler, J. Chem. Phys. **66**, 4707 (1977), and **69**, 725 (1978).

<sup>5</sup>W. I. Goldberg, C. H. Shaw, J. S. Hunag, and M. S. Pilant, J. Chem. Phys. **68**, 484 (1978).

<sup>6</sup>Y. C. Chou and W. I. Goldberg, Phys. Rev. A **20**, 2105 (1979).

<sup>7</sup>N. C. Wong and C. M. Knobler, Phys. Rev. Lett. **43**, 1733 (1979).

<sup>8</sup>K. N. Zinov'eva, Zh. Eksp. Teor. Fiz. **44**, 1837 (1963) [Sov. Phys. JETP **17**, 1235 (1963)].

<sup>9</sup>We call  $^3\text{He}$ - $^4\text{He}$  dispersions normal or superfluid according to the state of the majority, or continuous,

phase. Thus, the *dispersed phase* of the normal dispersion consists of  $^4\text{He}$ -rich droplets, which may or may not be superfluid, depending on their size and temperature.

<sup>10</sup>L. D. Landau and E. M. Lifshitz, *Fluid Mechanics* (Pergamon, London, 1959), p. 70.

<sup>11</sup>H. A. Kierstead, *J. Low Temp. Phys.* **24**, 497 (1976).

<sup>12</sup>C. M. Lai and T. A. Kitchens, in *Low Temperature Physics, LT-13*, edited by K. D. Timmerhaus, W. J. O'Sullivan, and E. F. Hammel (Plenum, New York, 1974), Vol. 1, p. 576.

<sup>13</sup>P. Leiderer, D. R. Watts, and W. W. Webb, *Phys.*

*Rev. Lett.* **33**, 483 (1974); P. Leiderer, D. R. Nelson, D. R. Watts, and W. W. Webb, *Phys. Rev. Lett.* **34**, 1080 (1975).

<sup>14</sup>I. M. Lifshitz and V. V. Slyozov, *J. Phys. Chem. Solids* **19**, 35 (1961); J. S. Langer, *Ann. Phys. (N.Y.)* **65**, 53 (1971); K. Binder, *Phys. Rev. B* **15**, 4425 (1977); K. Kawasaki and T. Ohta, *Prog. Theor. Phys.* **59**, 362 (1978).

<sup>15</sup>E. D. Siggia, *Phys. Rev. A* **20**, 595 (1979).

<sup>16</sup>L. J. Campbell, Y. Disatnik, and R. M. Ziff, Los Alamos Scientific Laboratory Report No. LA-7192-PR, 1978 (unpublished).

## Atomic Hydrogen in Contact with a Helium Surface: Bose Condensation, Adsorption Isotherms, and Stability

Isaac F. Silvera and Victor V. Goldman

*Natuurkundig Laboratorium der Universiteit van Amsterdam, 1018-XE Amsterdam, The Netherlands*

(Received 19 May 1980)

The energy of interacting spin-polarized atomic hydrogen ( $\text{H}_\uparrow$ ) on a helium surface and the density dependence of the adsorption energy have been calculated, permitting a realistic determination of the adsorption isotherms. Surface interactions are shown to allow Bose-Einstein condensation in the gas. At the Bose-Einstein condensation the surface coverage attains a maximum which is essentially independent of the isotherm temperature. Also calculated is the stability condition for surfaces in magnetic fields. Easily met requirements are found.

PACS numbers: 67.70.+n, 67.40.-w

A gas of spin-polarized atomic hydrogen ( $\text{H}_\uparrow$ ) has recently been stabilized to densities of order  $10^{16}$ – $10^{17}$  atoms/cm<sup>3</sup>.<sup>1</sup> This gas is only stable in a container with helium-covered walls. At densities a few orders of magnitude higher it is expected that the critical temperature [ $T_c \approx 3.31 \times \hbar^2/mk_B(n_3/g)^{2/3}$ ;  $n_3$  is the gas density,  $g$  the degeneracy, and  $m$  the mass] for Bose-Einstein condensation (BEC) will be within the range of current cryogenic techniques. The combination of the statistical attraction of bosons and the  $\text{H}_\uparrow$ - $\text{H}_\uparrow$  interactions leads to important phenomena. In the absence of interactions the surface coverage,  $n_2$ , becomes infinite at a critical density and no BEC will occur in the gas-surface system.<sup>2</sup> In this Letter we point out how interactions change this picture so that even at  $T=0$  K surface coverages are strongly limited. We calculate the  $T=0$  adsorption isotherm and extend this to finite temperatures. We find that for temperatures and densities of current experimental interest ( $0 \leq T \leq 0.5$  K,  $n_3 \leq 10^{21}$  atoms/cm<sup>3</sup>) there is a maximum surface coverage which is essentially independent of temperature. Moreover, our results show that

this maximum coverage must be reached on the surface before BEC can be observed at the critical density  $n_3 = n_{3c}$ . For experimental efforts to observe BEC in  $\text{H}_\uparrow$ , there is thus no optimum temperature to minimize recombination to  $\text{H}_2$  on the surface. We also calculate the magnetic field value required to provide static stability against recombination both in the gas and on the helium surface. We find that experimentally available fields are sufficient to achieve static stability of  $\text{H}_\uparrow$  at  $n_{3c}$  and the predicted maximum value of  $n_2$ .

We first show that another of the unique properties of  $\text{H}_\uparrow$  in equilibrium with a helium surface is that it has a nontrivial isotherm at  $T=0$  K; i.e., above a critical coverage the gas has a finite pressure and density. We consider a two-dimensional (2D) gas of  $\text{H}_\uparrow$  with surface density  $n_2$  adsorbed on helium in equilibrium with a 3D gas of  $\text{H}_\uparrow$  with density  $n_3$ . The isotherm is obtained by requiring the equality of the chemical potentials  $\mu_2$  and  $\mu_3$  of the surface-gas system. To determine the energy  $\epsilon$  as a function of coverage we assume that motions within and normal to the surface are uncoupled so that they are additive:  $\epsilon$

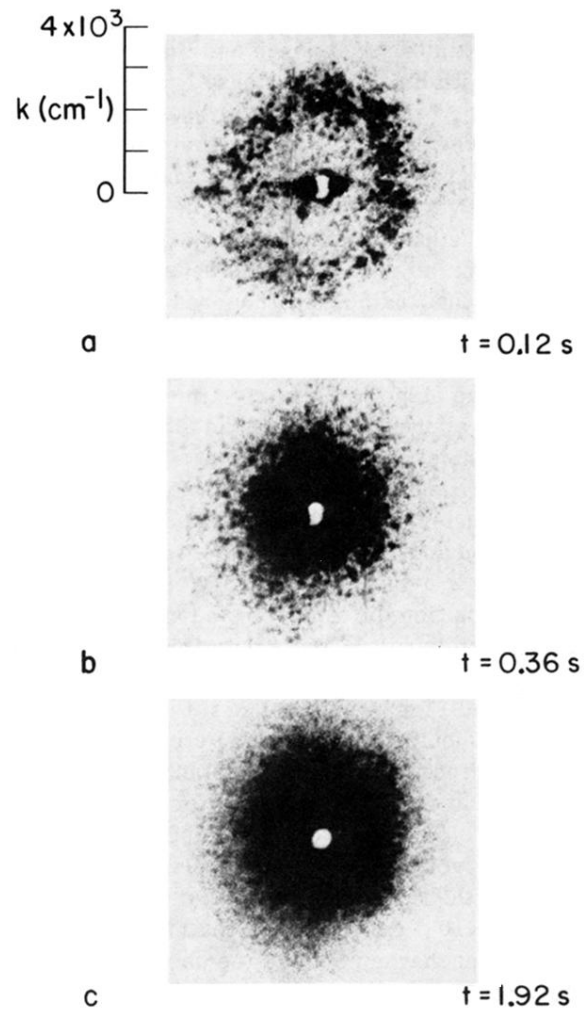


FIG. 2. Far-field scattering of laser beam at three times after decompression from a state represented by the upper open dot in Fig. 1. The center spot is a hole in the screen to pass the undeflected beam.